PERGAMON

International Journal of Solids and Structures 39 (2002) 2547–2556

INTERNATIONAL JOURNAL OF SOLIDS and STRUCTURES

www.elsevier.com/locate/ijsolstr

Lamb wave propagation in a metallic semi-infinite medium covered with piezoelectric layer

J. Jin, Q. Wang *, S.T. Quek

Department of Civil Engineering, National University of Singapore, 1 Engineering Drive 2, 117576 Singapore, Singapore

Received 26 April 2001; received in revised form 29 November 2001

Abstract

The Lamb wave propagation in a metallic semi-infinite medium covered with a piezoelectric layer is studied in this paper. The numerical solution of the dispersion curve is simplified by segmenting the phase velocity spectrum into different ranges based on the longitudinal and transverse wave velocities of both materials, and using different forms of wave equations. The results show that the dispersion curves are asymptotic to the transverse velocity of the piezoelectric layer as the wave number increases. The first two mode shapes of the electric potential correspond to a half-cosine distribution at low wave number and a full-sinusoidal distribution at relatively higher wave number.

Keywords: Lamb wave; Piezoelectric material; Dispersion characteristics; Mode shapes; Structure analysis

1. Introduction

Vibration and wave propagation in pure piezoelectric solids have received considerable attention previously as exhibited by the works of Mindlin (1952), Tiersten (1963a,b), Bleustein (1969), and Cheng and Sun (1975). The availability of piezoelectric materials with strong electromechanical coupling resulted in the growing application and demand for new control elements involving piezoelectric devices as sensors and actuators. Examples include piezoelectric ultrasonic motors, piezoelectric transducers in the application of structural health monitoring, and vibration control or noise suppression with piezoelectric layer. Subsequently, the coupling effects between the piezoelectric material and the host material become a topic of practical importance (Crawley and de Luis, 1987; Lee and Moon, 1989; Sun and Zhang, 1995; Varadan et al., 1996).

The acoustic wave propagating in solids can be decoupled into two kinds of waves, namely, SH wave and Lamb wave (Viktorov, 1967; Graff, 1975). When piezoelectric material is employed in solid structure, the dispersive characteristics of both waves will be affected by the electromechanical coupling. Hence, the piezoelectric characteristics must be considered in the analytic model (Lamberti and Pappalardo, 1989;

* Corresponding author.
E-mail address: cvewangq@nus.edu.sg (Q. Wang).

0020-7683/02/$ - see front matter
PII: S0020-7683(02)00091-4

Nayfeh and Chien, 1992; Laprus and Danicki, 1997; Nayfeh et al., 2000). The SH wave propagating in piezoelectric layered structures has been investigated recently by Wang et al. (2001) and Liu et al. (2001), respectively. The Lamb wave propagating in such structures will be addressed in this paper. An accurate model for the piezoelectric effect in a coupled structure is essential to the application of piezoelectric materials as sensors and actuators. Fundamental to wave propagation studies would be the dispersive characteristics of waves affected by the electromechanical effects. Furthermore, the mode shapes of the electric potential distribution in the thickness direction of the piezoelectric layer will be derived and compared with the assumed electric potential distribution in the various models used in vibration analysis (Krommer and Irschik, 1999; Gopinathan et al., 2000).

2. Formulation of dispersion equation in coupled structure

Consider the wave propagation in a structure comprising a metallic semi-infinite medium with a piezoelectric layer of thickness H perfectly bonded on it as shown in Fig. 1. Continuity of displacements and stresses between the layer and the semi-infinite medium is thus implied. The top surface of the piezoelectric layer is free from tractions and electrically shorted. The piezoelectric relations are assumed linear and quasi-stationary electric field is considered.

2.1. Governing equations

In rectangular Cartesian coordinates, the stress equations of motion are given by

$$\sum_{j=1}^{3} T_{ij,j} = \rho \ddot{u}_i \tag{1}$$

for $i = 1$, 2 and 3, where T_{ij} is the stress tensor, u_i the mechanical displacement, ρ the mass density, and subscript "j" indicates differentiation with respect to x_j. The electric displacement D_i satisfies Maxwell's equation,

$$\sum_{i=1}^{3} D_{i,i} = 0. \tag{2}$$

The electric field E_i (for $i = 1$, 2 and 3) is related to the electric potential ϕ by

$$E_i = -\phi_{,i}. \tag{3}$$

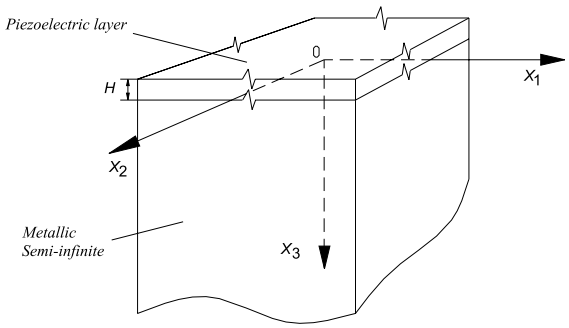

Fig. 1. Piezoelectric layered semi-infinite structure.

The constitutive equations are different for different dependent on the types of piezoelectric materials considered. In this paper, the piezoelectric material of hexagon crystal structure, class 6 mm, is employed. For other types of piezoelectric material, the constitutive equations should be changed accordingly. Assuming the six-fold axes of the piezoelectric material parallel to the x_3-direction, its constitutive equations can be expressed in the form

$$\begin{aligned}
T_{11} &= c_{11}S_{11} + c_{12}S_{22} + c_{13}S_{33} - e_{31}E_3,\\
T_{22} &= c_{12}S_{11} + c_{11}S_{22} + c_{13}S_{33} - e_{31}E_3,\\
T_{33} &= c_{13}S_{11} + c_{13}S_{22} + c_{33}S_{33} - e_{33}E_3,\\
T_{23} &= c_{44}S_{23} - e_{15}E_2,\\
T_{13} &= c_{44}S_{13} - e_{15}E_1,\\
T_{12} &= c_{66}S_{12} = 0.5(c_{11} - c_{12})S_{12},\\
D_1 &= e_{15}S_{13} + \varepsilon_{11}E_1,\\
D_2 &= e_{15}S_{23} + \varepsilon_{11}E_2,\\
D_3 &= e_{31}S_{11} + e_{31}S_{22} + e_{33}S_{33} + \varepsilon_{33}E_3,
\end{aligned} \tag{4}$$

where the coefficients c, e and ε are the elastic, piezoelectric and dielectric constants, and the strain components are defined as

$$S_{11} = u_{1,1} \quad S_{22} = u_{2,2} \quad S_{33} = u_{3,3} \quad S_{23} = u_{2,3} + u_{3,2} \quad S_{13} = u_{3,1} + u_{1,3} \quad S_{12} = u_{2,1} + u_{1,2}. \tag{5}$$

For other types of piezoelectric material, the constitutive equations should be changed accordingly.

It is assumed that a state of plane strain parallel to the x_2–x_3 (or x_1–x_3) plane exists and the propagation of waves in the x_2-direction (or x_1-direction) is considered. Substituting Eqs. (3)–(5) in Eqs. (1) and (2), the electromechanical-coupled equations of motion in terms of the mechanical displacements and electric potential can be simplified as

$$\begin{aligned}
&c_{11}u_{2,22} + c_{44}u_{2,33} + (c_{13} + c_{44})u_{3,23} + (e_{31} + e_{15})\phi_{,23} = \rho\ddot{u}_2\\
&(c_{13} + c_{44})u_{2,32} + c_{44}u_{3,22} + c_{33}u_{3,33} + e_{15}\phi_{,22} + e_{33}\phi_{,33} = \rho\ddot{u}_3\\
&(e_{15} + e_{31})u_{2,23} + e_{15}u_{3,22} + e_{33}u_{3,33} - \varepsilon_{11}\phi_{,22} - \varepsilon_{33}\phi_{,33} = 0.
\end{aligned} \tag{6}$$

The governing equation for the metallic material can be obtained by setting the piezoelectric and dielectric constants in Eq. (6) to zero, giving

$$\begin{aligned}
&c'_{11}u_{2,22} + c'_{44}u_{2,33} + (c'_{13} + c'_{44})u_{3,23} = \rho'\ddot{u}_2\\
&(c'_{13} + c'_{44})u_{2,32} + c'_{44}u_{3,22} + c'_{33}u_{3,33} = \rho'\ddot{u}_3.
\end{aligned} \tag{7}$$

where the material properties of the metallic semi-infinite are differentiate with the prime notation throughout this paper.

2.2. Wave motion equations in the piezoelectric layer

Consider the free wave propagation in the x_2-direction, expressed in the form (Cheng and Sun, 1975)

$$\begin{aligned}
u_2 &= A\mathrm{e}^{bkx_3}\cos k(x_2 - vt),\\
u_3 &= B\mathrm{e}^{bkx_3}\sin k(x_2 - vt),\\
\phi &= C\mathrm{e}^{bkx_3}\sin k(x_2 - vt),
\end{aligned} \tag{8}$$

where k is the angular wave number, v the phase velocity, A, B and C are constants, and b is a parameter to be determined.

Substituting Eq. (8) in Eq. (6) yields

$$\begin{bmatrix} (c_{44}b^2 - c_{11} + \rho v^2) & (c_{13} + c_{44})b & (e_{15} + e_{31})b \\ (c_{13} + c_{44})b & (c_{44} - c_{33}b^2 - \rho v^2) & (e_{15} - e_{33}b^2) \\ (e_{15} + e_{31})b & (e_{15} - e_{33}b^2) & (\varepsilon_{33}b^2 - \varepsilon_{11}) \end{bmatrix} \begin{pmatrix} A \\ B \\ C \end{pmatrix} = A[K] \begin{pmatrix} 1 \\ \alpha \\ \beta \end{pmatrix} = 0, \tag{9}$$

where a non-trivial solution for A, B and C (or A, α and β) requires that

$$|K| = 0. \tag{10}$$

For a value of v there are six roots for b, each root represents one component propagating in the piezoelectric layer and yields a partial solution to the piezoelectric layer.

It can be shown that for $v < v_2$, where $v_2 = \sqrt{(c_{44} + e_{15}^2/\varepsilon_{11})/\rho}$ = transverse mode wave propagation velocity in piezoelectric layer, only two of the six roots of b in Eq. (10) are real and the other four roots contain both real and imaginary parts and hence not valid for harmonic wave propagation in the piezoelectric layer (Parton and Kudryavtsev, 1988). For $v \geqslant v_2$, the roots of b are either real or imaginary, taking the form $(\pm p_1\mathrm{i}, \pm p_2, \pm p_3)$ for $v_2 \leqslant v < v_1$ or $(\pm p_1\mathrm{i}, \pm p_2\mathrm{i}, \pm p_3)$ for $v \geqslant v_1$, where $v_1 = \sqrt{c_{11}/\rho}$ = longitudinal mode wave propagation velocity and p_i, $i = 1, 2, 3$ are positive and real. The real and imaginary roots correspond to the non-propagating and propagating wave components respectively.

For ease of numerical solution by eliminating complex manipulation, Eq. (8) can be re-written in the following two form. For $v_2 \leqslant v < v_1$,

$$\begin{aligned} u_2 &= (D_1 \sin p_1 kx_3 + D_2 \cos p_1 kx_3 + D_3 \mathrm{e}^{p_2 kx_3} + D_4 \mathrm{e}^{-p_2 kx_3} + D_5 \mathrm{e}^{p_3 kx_3} + D_6 \mathrm{e}^{-p_3 kx_3}) \cos k(x_2 - vt), \\ u_3 &= (D_1\alpha_1 \cos p_1 kx_3 + D_2\alpha_2 \sin p_1 kx_3 + D_3\alpha_3 \mathrm{e}^{p_2 kx_3} + D_4\alpha_4 \mathrm{e}^{-p_2 kx_3} + D_5\alpha_5 \mathrm{e}^{p_3 kx_3} + D_6\alpha_6 \mathrm{e}^{-p_3 kx_3}) \sin k(x_2 - vt), \\ \phi &= (D_1\beta_1 \cos p_1 kx_3 + D_2\beta_2 \sin p_1 kx_3 + D_3\beta_3 \mathrm{e}^{p_2 kx_3} + D_4\beta_4 \mathrm{e}^{-p_2 kx_3} + D_5\beta_5 \mathrm{e}^{p_3 kx_3} + D_6\beta_6 \mathrm{e}^{-p_3 kx_3}) \sin k(x_2 - vt), \end{aligned} \tag{11}$$

where D_i, $i = 1$–6, are constants. The eigen-solutions $(p_i, \alpha_i, \beta_i, i = 3, 4, 5, 6)$ can be obtained from Eq. (9) whereas (p_1, α_1, β_1) and (p_2, α_2, β_2) can be obtained respectively from the following equations

$$D \begin{bmatrix} (c_{44}b^2 + c_{11} - \rho v^2) & (c_{13} + c_{44})b & (e_{15} + e_{31})b \\ (c_{13} + c_{44})b & (c_{44} + c_{33}b^2 - \rho v^2) & (e_{15} + e_{33}b^2) \\ (e_{15} + e_{31})b & (e_{15} + e_{33}b^2) & (-\varepsilon_{33}b^2 - \varepsilon_{11}) \end{bmatrix} \begin{pmatrix} 1 \\ \alpha \\ \beta \end{pmatrix} = 0, \tag{12}$$

$$D \begin{bmatrix} -(c_{44}b^2 + c_{11} - \rho v^2) & (c_{13} + c_{44})b & (e_{15} + e_{31})b \\ -(c_{13} + c_{44})b & (c_{44} + c_{33}b^2 - \rho v^2) & (e_{15} + e_{33}b^2) \\ -(e_{15} + e_{31})b & (e_{15} + e_{33}b^2) & (-\varepsilon_{33}b^2 - \varepsilon_{11}) \end{bmatrix} \begin{pmatrix} 1 \\ \alpha \\ \beta \end{pmatrix} = 0. \tag{13}$$

For $v \geqslant v_1$,

$$\begin{aligned} u_2 &= (D_1 \sin p_1 kx_3 + D_2 \cos p_1 kx_3 + D_3 \sin p_2 kx_3 + D_4 \cos p_2 kx_3 + D_5 \mathrm{e}^{p_3 kx_3} + D_6 \mathrm{e}^{-p_3 kx_3}) \cos k(x_2 - vt), \\ u_2 &= (D_1\alpha_1 \cos p_1 kx_3 + D_2\alpha_2 \sin p_1 kx_3 + D_3\alpha_3 \cos p_2 kx_3 + D_4\alpha_4 \sin p_2 kx_3 + D_5\alpha_3 \mathrm{e}^{p_3 kx_3} + D_6\alpha_3 \mathrm{e}^{-p_3 kx_3}) \\ &\quad \times \sin k(x_2 - vt), \\ u_2 &= (D_1\beta_1 \cos p_1 kx_3 + D_2\beta_2 \sin p_1 kx_3 + D_3\beta_3 \cos p_2 kx_3 + D_4\beta_4 \sin p_2 kx_3 + D_5\beta_3 \mathrm{e}^{p_3 kx_3} + D_6\beta_3 \mathrm{e}^{-p_3 kx_3}) \\ &\quad \times \sin k(x_2 - vt), \end{aligned} \tag{14}$$

where the eigen-solutions (p_1, α_1, β_1) and (p_3, α_3, β_3) can be obtained from Eq. (12), (p_2, α_2, β_2) and (p_4, α_4, β_4) from Eq. (13), and (p_5, α_5, β_5) and (p_6, α_6, β_6) from Eq. (9).

2.3. Wave motion equations in the metallic semi-infinite medium

Similarly, the free wave propagation in the x_2-direction in the metallic semi-infinite medium can be expressed in the form

$$\begin{aligned} u_2' &= A' e^{b' k x_3} \cos k(x_2 - vt), \\ u_3' &= B' e^{b' k x_3} \sin k(x_2 - vt). \end{aligned} \tag{15}$$

Substituting Eq. (15) into Eq. (7) yields

$$\begin{bmatrix} (c_{44}' b'^2 - c_{11}' + \rho' v^2) & (c_{13}' + c_{44}') b' \\ (c_{13}' + c_{44}') b' & (c_{44}' - c_{33}' b'^2 - \rho' v^2) \end{bmatrix} \begin{pmatrix} A' \\ B' \end{pmatrix} = A' [K'] \begin{pmatrix} 1 \\ \alpha' \end{pmatrix} = 0. \tag{16}$$

For a value of v, there are four roots for b' from the equation

$$|K'| = 0. \tag{17}$$

Depending on v, these four roots can take three different forms, namely, $b' = (\pm p_1', \pm p_2')$ or $(\pm p_1' \mathrm{i}, \pm p_2')$ or $(\pm p_1' \mathrm{i}, \pm p_2' \mathrm{i})$, where p_1' and p_2' are positive and real. The three forms correspond respectively to $v < v_2'$, $v_2' \leqslant v < v_1'$ and $v \geqslant v_1'$, where $v_1' = \sqrt{c_{11}'/\rho'}$ = longitudinal mode wave velocity, $v_2' = \sqrt{c_{44}'/\rho'}$ = transverse mode wave velocity, and $v_1' > v_2'$. The components $e^{-p_i' \mathrm{i} k x_3}$ represent wave moving in the negative x_3-direction whereas the case considered here is from the piezoelectric layer in the positive x_3-direction. The components $e^{p_i' k x_3}$ represent wave energy increases to infinity as x_3 increases. Both cases should be discarded and only two roots, namely $b' = (-p_1', -p_2')$ or $(p_1' \mathrm{i}, -p_2')$ or $(p_1' \mathrm{i}, p_2' \mathrm{i})$, are of interest for harmonic wave propagation in the metallic semi-infinite medium.

For ease of numerical solution by eliminating complex manipulation, Eq. (15) can be re-written in the following two form. For $v < v_2'$,

$$\begin{aligned} u_2' &= [D_1' e^{-p_1' k x_3} + D_2' e^{-p_2' k x_3}] \cos k(x_2 - vt), \\ u_3' &= [D_1' \alpha_1' e^{-p_1' k x_3} + D_2' \alpha_2' e^{-p_2' k x_3}] \sin k(x_2 - vt), \end{aligned} \tag{18}$$

where D_1', D_2' are constants. The eigen-solutions (p_1', α_1') and (p_2', α_2') can be obtained from Eq. (16).

For $v_2' \leqslant v < v_1'$,

$$\begin{aligned} u_2' &= [D_1' \sin(p_1' k x_3) + D_1' \cos(p_1' k x_3) + D_2' e^{-p_2' k x_3}] \cos k(x_2 - vt), \\ u_3' &= [D_1' \alpha_1' \cos(p_1' k x_3) + D_1' \alpha_2' \sin(p_1' k x_3) + D_2' \alpha_3' e^{-p_2' k x_3}] \sin k(x_2 - vt), \end{aligned} \tag{19}$$

where (p_1', α_1') and (p_2', α_2') can be obtained respectively from the following equations

$$D' \begin{bmatrix} (c_{44}' b'^2 + c_{11}' - \rho' v^2) & (c_{13}' + c_{44}') b' \\ (c_{13}' + c_{44}') b' & (c_{44}' + c_{33}' b'^2 - \rho' v^2) \end{bmatrix} \begin{pmatrix} 1 \\ \alpha' \end{pmatrix} = 0, \tag{20}$$

$$D' \begin{bmatrix} -(c_{44}' b'^2 + c_{11}' - \rho' v^2) & (c_{13}' + c_{44}') b' \\ -(c_{13}' + c_{44}') b' & (c_{44}' + c_{33}' b'^2 - \rho' v^2) \end{bmatrix} \begin{pmatrix} 1 \\ \alpha' \end{pmatrix} = 0 \tag{21}$$

and (p_3', α_3') from Eq. (16).

For $v \geqslant v_1'$,

$$\begin{aligned} u_2' &= [D_1' \sin(p_1' k x_3) + D_1' \cos(p_1' k x_3) + D_2' \sin(p_2' k x_3) + D_2' \cos(p_2' k x_3)] \cos k(x_2 - vt), \\ u_3' &= [D_1' \alpha_1' \cos(p_1' k x_3) + D_1' \alpha_2' \sin(p_1' k x_3) + D_2' \alpha_3' \cos(p_2' k x_3) + D_2' \alpha_4' \sin(p_2' k x_3)] \sin k(x_2 - vt), \end{aligned} \tag{22}$$

where (p_1', α_1') and (p_3', α_3') can be obtained from Eq. (20), and (p_2', α_2') and (p_4', α_4') from Eq. (21).

2.4. Boundary conditions

The top surface of the piezoelectric layer is traction-free and electrically shorted, that is, at $x_3 = -H$,

$$T_{33} = T_{23} = \phi = 0. \tag{23}$$

The interface between the piezoelectric layer and metallic medium is electrically shorted since the latter is semi-infinite. Hence at $x_3 = 0$,

$$\phi = 0. \tag{24}$$

The continuity conditions at the interface $x_3 = 0$ can be written as

$$\begin{aligned} &u_2 = u_2' \quad u_3 = u_3', \\ &T_{33} = T_{33}' \quad T_{23} = T_{23}'. \end{aligned} \tag{25}$$

2.5. Wave dispersion equations

Substituting Eq. (11) or (14) and Eq. (18) or (19) or (22) into boundary conditions Eqs. (23)–(25), in view of Eqs. (4) and (5), yield six different sets of eight homogeneous equations for D_i, $i = 1$–6 and D_i' $(i = 1, 2)$. The dispersion equations could be obtained using the non-trivial solution condition.

The six sets can be further reduced depending on the properties of the semi-infinite medium and the piezoelectric layer. For PZT-4 and aluminum, $v_2 < v_2' < v_1 < v_1'$ and coupled with the condition $v \geqslant v_2$ gives only four different sets of eight homogeneous equations.

For $v_2 \leqslant v < v_2'$, the wave in the PZT-4 layer consists of two propagating components ($b = \pm p_1\mathrm{i}$) and four non-propagating components ($b = \pm p_2, \pm p_3$) while the wave in the aluminum medium comprises two non-propagating components ($b' = -p_1', -p_2'$). Using Eqs. (11) and (18), the resultant system of eight equations can be written as

$$\begin{aligned} &-D_1(c_{13} + c_{33}\alpha_1 p_1 + e_{33}\beta_1 p_1)\sin p_1 kH + D_2(c_{13} - c_{33}\alpha_2 p_1 - e_{33}\beta_2 p_1)\cos p_1 kH \\ &\quad + D_3(c_{13} - c_{33}a_3 p_2 - e_{33}\beta_3 p_2)\mathrm{e}^{-p_2 kH} + D_4(c_{13} + c_{33}\alpha_4 p_2 + e_{33}\beta_4 p_2)\mathrm{e}^{p_2 kH} \\ &\quad + D_5(c_{13} - c_{33}\alpha_5 p_3 - e_{33}\beta_5 p_3)\mathrm{e}^{-p_3 kH} + D_6(c_{13} + c_{33}\alpha_6 p_3 + e_{33}\beta_6 p_3)\mathrm{e}^{p_3 kH} = 0, \end{aligned} \tag{26a}$$

$$\begin{aligned} &D_1(c_{44}p_1 + c_{44}\alpha_1 + e_{15}\beta_1)\cos p_1 kH - D_2(-c_{44}p_1 + c_{44}\alpha_2 + e_{15}\beta_2)\sin p_1 kH \\ &\quad + D_3(c_{44}p_2 + c_{44}\alpha_3 + e_{15}\beta_3)\mathrm{e}^{-p_2 kH} + D_4(-c_{44}p_2 + c_{44}\alpha_4 + e_{15}\beta_4)\mathrm{e}^{p_2 kH} \\ &\quad + D_5(c_{44}p_3 + c_{44}\alpha_5 + e_{15}\beta_5)\mathrm{e}^{-p_3 kH} + D_6(-c_{44}p_3 + c_{44}\alpha_6 + e_{15}\beta_6)\mathrm{e}^{p_3 kH} = 0, \end{aligned} \tag{26b}$$

$$D_1\beta_1\cos p_1 kH - D_2\beta_2\sin p_1 kH + D_3\beta_3\mathrm{e}^{-p_2 kH} + D_4\beta_4\mathrm{e}^{p_2 kH} + D_5\beta_5\mathrm{e}^{-p_3 kH} + D_6\beta_6\mathrm{e}^{p_3 kH} = 0, \tag{26c}$$

$$D_1\beta_1 + D_3\beta_3 + D_4\beta_4 + D_5\beta_5 + D_6\beta_6 = 0, \tag{26d}$$

$$D_2 + D_3 + D_4 + D_5 + D_6 - D_1' - D_2' = 0, \tag{26e}$$

$$D_1\alpha_1 + D_3\alpha_3 + D_4\alpha_4 + D_5\alpha_5 + D_6\alpha_6 - D_1'\alpha_1' - D_2'\alpha_2' = 0, \tag{26f}$$

$$\begin{aligned} &D_2(c_{13} - c_{33}\alpha_2 p_1 - e_{33}\beta_2 p_1) + D_3(c_{13} - c_{33}a_3 p_2 - e_{33}\beta_3 p_2) + D_4(c_{13} + c_{33}\alpha_4 p_2 + e_{33}\beta_4 p_2) \\ &\quad + D_5(c_{13} - c_{33}\alpha_5 p_3 - e_{33}\beta_5 p_3) + D_6(c_{13} + c_{33}\alpha_6 p_3 + e_{33}\beta_6 p_3) - D_1'(c_{13}' + c_{33}'\alpha_1' p_1') - D_2'(c_{13}' + c_{33}'\alpha_2' p_2') = 0, \end{aligned} \tag{26g}$$

$$D_1(c_{44}p_1 + c_{44}\alpha_1 + e_{15}\beta_1) + D_3(c_{44}p_2 + c_{44}\alpha_3 + e_{15}\beta_3) + D_4(-c_{44}p_2 + c_{44}\alpha_4 + e_{15}\beta_4) + D_5(c_{44}p_3 + c_{44}\alpha_5 + e_{15}\beta_5) + D_6(-c_{44}p_3 + c_{44}\alpha_6 + e_{15}\beta_6) - D'_1c'_{44}(-p'_1 + \alpha'_1) - D'_2c'_{44}(-p'_2 + \alpha'_2) = 0. \tag{26h}$$

Let the coefficient matrix be denoted as R_{mn}, where $m, n = 1$–8. The wave dispersion equation can be obtained by imposing the non-trivial solution condition, that is,

$$|R_{mn}| = 0. \tag{27}$$

Thus, for a given value of phase velocity v, the wave number k is solved through Eq. (27). Similar equations can be written for the remaining three ranges of v.

For $v'_2 \leqslant v < v_1$, the wave in the PZT-4 layer consists of two propagating components ($b = \pm p_1\mathrm{i}$) and four non-propagating components ($b = \pm p_2, \pm p_3$) while the wave in the aluminum medium comprises one propagating component ($b' = p'_1\mathrm{i}$) and one non-propagating component ($b' = -p'_2$). Eqs. (11) and (19) are used to obtain the resultant system of eight equations.

For $v_1 \leqslant v < v'_1$, the wave in the PZT-4 layer consists of four propagating components ($b = \pm p_1\mathrm{i}, \pm p_2\mathrm{i}$) and two non-propagating components ($b = \pm p_3$) while the wave in the aluminum medium comprises one propagating component ($b' = p'_1\mathrm{i}$) and one non-propagating component ($b' = -p'_2$). Hence, Eqs. (14) and (19) are used.

For $v'_1 \leqslant v$, the wave in the PZT-4 layer consists of four propagating components ($b = \pm p_1\mathrm{i}, \pm p_2\mathrm{i}$) and two non-propagating components ($b = \pm p_3$) while the wave in the aluminum medium comprises two propagating components ($b' = p'_1\mathrm{i}$, $p'_2\mathrm{i}$). Hence, Eqs. (14) and (22) are used.

For a given value of v, the eigen-solution (kH, D_i, D'_i) can be obtained from one of the above four sets of equations where kH is the wave number, non-dimensionalised by the thickness of the piezoelectric layer. The shape of the distribution of displacements and potentials inside the piezoelectric layer is obtained subsequently from Eq. (11) or (14) and that of the displacements inside the metallic semi-infinite from Eqs. (18), (19) or (22).

3. Numerical results

Using the material properties given in Table 1, the dispersion curves of the first five modes obtained based on the four phase velocity ranges are shown to be continuous in Fig. 2. The phase velocities for the five modes are asymptotic to the transverse velocity v_2 of the piezoelectric layer as the product kH increases

Table 1
Material properties of PZT-4 and aluminum

	PZT	Aluminum
ρ ($\times 10^3$ kg/m^3)	7.5	2.7
c_{11} ($\times 10^{10}$ N/m^2)	13.2	10.2
c_{33} ($\times 10^{10}$ N/m^2)	11.5	10.2
c_{44} ($\times 10^{10}$ N/m^2)	2.6	2.6
c_{12} ($\times 10^{10}$ N/m^2)	7.1	5.0
c_{13} ($\times 10^{10}$ N/m^2)	7.3	5.0
e_{15} (C/m^2)	10.5	–
e_{33} (C/m^2)	14.1	–
e_{31} (C/m^2)	−4.1	–
ε_{11} ($\times 10^{-9}$ F/m)	7.1	–
ε_{33} ($\times 10^{-9}$ F/m)	5.8	–
v_1 ($\times 10^3$ m/s)	4.2	6.2
v_2 ($\times 10^3$ m/s)	2.4	3.1

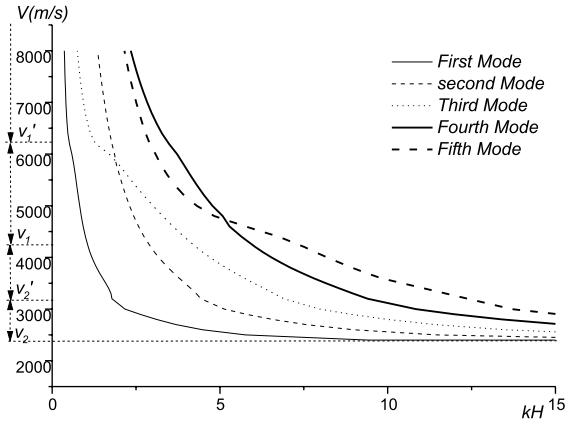

Fig. 2. Dispersion curves of the first five modes from four phase velocity ranges.

and increase to infinity as the product kH approaches zero. This phenomenon can be observed in most dispersion curves of various wave propagation problems. Because the wavelength approaches infinity as the product kH approaches zero, it takes almost no time for the wave to travel inside the structure, that is, the phase velocity approaches infinity.

Figs. 3–5 are the first three mode shapes of the electric potential distribution along x_3-direction in the piezoelectric layer at different wave numbers, respectively. For easy comparison, the electric potential is normalized by setting the largest value in each curve equal to 1 or -1. In Fig. 3, the first mode shape of the electric potential at small wave number (kH is approximately 0.75) follows a half-cosine distribution. As kH increases, the first mode shape distorts into a combination of a half-cosine and a full-cycle sine distribution and approaches a full-cycle sinusoidal distribution when kH reaches a relatively higher value ($\approx$1.75). As kH increases further, the mode shape continues to distort. It can be seen from Fig. 4 that the same trend is observed for the second mode shape of the electric potential. The demarcating kH values are $\approx$0.75 and 2.5, respectively. However, the higher mode shapes are much more complicated, as depicted by the third mode shape shown in Fig. 5. The potential distribution of the third mode shape at $kH = 0.75$ is not depicted because the corresponding velocity is too large for numerical calculation, as illustrated in Fig. 2. The first

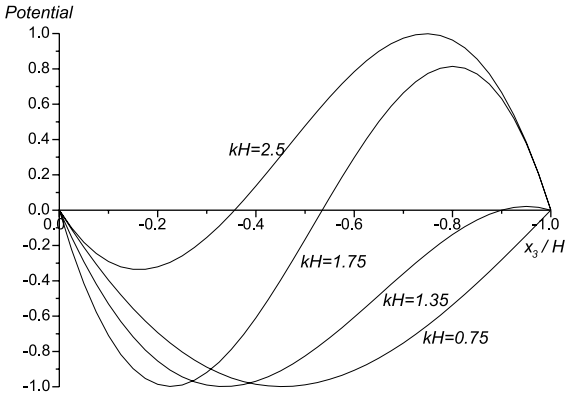

Fig. 3. Distribution of potential of first mode shape along x_3-direction in the piezoelectric layer for different wave numbers.

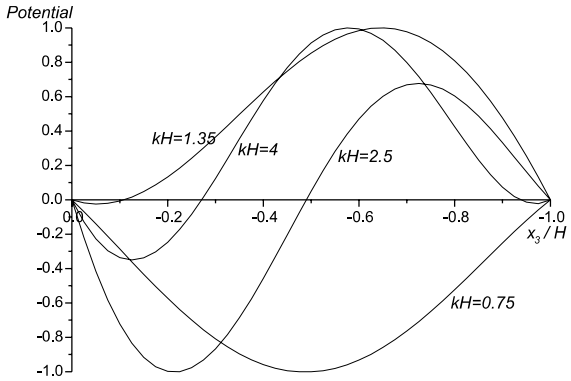

Fig. 4. Distribution of potential of second mode shape along x_3-direction in the piezoelectric layer for different wave numbers.

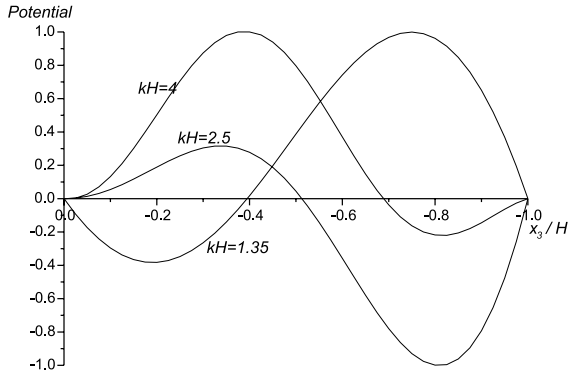

Fig. 5. Distribution of potential of third mode shape along x_3-direction in the piezoelectric layer for different wave numbers.

two mode shapes of electric potential displaying a half-cosine distribution at small wave number is consistent with the results of the SH wave propagation for the same structure (Wang et al., 2001).

In vibration analysis, only the basic modes are of interests, the assumption of half cosine distribution of potential is valid at small wave number. However the more precise model is a combination of a cosine distribution and a full-cycle sine distribution for higher frequency consideration.

4. Conclusion

The Lamb wave propagation in a metallic semi-infinite medium covered with a piezoelectric layer is studied. Due to the electromechanical coupling effect of the layered structure, the numerical solution of the characteristics of wave components propagating inside the piezoelectric layer and the semi-infinite medium becomes complex. It is shown that by using different forms of wave equations and segmenting the phase velocity spectrum into different ranges, continuous dispersion curves can be obtained. The dispersion curves are asymptotic to the transverse velocity of the piezoelectric layer. The first two mode shapes of the electric potential distribution along x_3-direction in the piezoelectric layer correspond to a half-cosine distribution at low wave number and a full-sinusoidal distribution at higher wave number.

Acknowledgements

The authors are indebted to the reviewers for their constructive suggestions, which do help to improve the quality of this paper. The financial support provided by the National University of Singapore for carrying out this study is appreciated.

References

Bleustein, J.L., 1969. Some simple modes of wave propagation in an infinite piezoelectric plate. Journal Acoustics Society of America 45, 614–620.

Crawley, E.F., de Luis, J., 1987. Use of piezoelectric actuators as elements of intelligent structures. AIAA Journal 25, 1373–1385.

Cheng, N.C., Sun, C.T., 1975. Wave propagation in two-layered piezoelectric plates. Journal Acoustics Society of America 57, 632–638.

Gopinathan, S.V., Varadan, V.V., Varadan, V.K., 2000. A review and critique of theories for piezoelectric laminates. Smart Materials and Structures 9, 24–48.

Graff, K.F., 1975. Wave Motion in Elastic Solids. Dover, New York.

Krommer, M., Irschik, H., 1999. On the influence of the electric field on free transverse vibrations of smart beams. Smart Materials and Structures 8, 401–410.

Lamberti, N., Pappalardo, M., 1989. Two-dimensional model for bounded resonant piezoelectric ceramic plate. Ultrasonics Symposium Proceedings 2, 775–779.

Laprus, W., Danicki, E., 1997. Piezoelectric interfacial waves in lithium niobate and other crystals. Journal of Applied Physics 81, 855–861.

Lee, C.K., Moon, F.C., 1989. Laminated piezopolymer plates for torsion and bending sensors and actuators. Journal of Acoustics Society of America 85, 2432–2439.

Liu, H., Wang, Z.K., Wang, T.J., 2001. Effect of initial stress on the propagation behavior of Love waves in a layered piezoelectric structure. International Journal of Solids and Structures 38, 7–51.

Mindlin, R.D., 1952. Forced thickness-shear and flexural vibrations of piezoelectric crystal plates. Journal of Applied Physics 23, 83–88.

Nayfeh, A.H., Abdelrahman, W.G., Nagy, P.B., 2000. Analyses of axisymmetric waves in layered piezoelectric rods and their composites. Journal of the Acoustical Society of America 108, 1496–1504.

Nayfeh, A.H., Chien, H.T., 1992. Wave propagation interaction with free and fluid-loaded piezoelectric substrates. Journal of the Acoustical Society of America 91, 3126–3135.

Parton, V.Z., Kudryavtsev, B.A., 1988. Electromagnetoelasticity: Piezoelectrics and Electrically Conductive Solids. Gordon & Breach, NY.

Sun, C.T., Zhang, X.D., 1995. Use of thickness shear mode in adaptive sandwich structures. Smart Materials and Structures 4, 202–206.

Tiersten, H.F., 1963a. Thickness vibrations of piezoelectric plates. Journal Acoustics Society of America 35, 53–58.

Tiersten, H.F., 1963b. Wave propagation in an infinite piezoelectric plate. Journal Acoustics Society of America 35, 234–239.

Varadan, V.K., Lim, Y.H., Varadan, V.V., 1996. Close loop finite element modeling of active/passive damping in structural vibration control. Smart Materials and Structures 5, 685–694.

Viktorov, I.A., 1967. Rayleigh and Lamb Waves. Plenum, New York.

Wang, Q., Quek, S.T., Varadan, V.K., 2001. Love wave in piezoelectric coupled solid media. Smart Materials and Structures 10, 380–388.